



# Capability of weld seam improvement techniques for the fatigue strength optimization of welded high strength steels

Tom Werner<sup>1</sup> · Thomas Nitschke-Pagel<sup>1</sup> · Klaus Dilger<sup>1</sup>

Received: 13 October 2022 / Accepted: 21 January 2023 / Published online: 7 March 2023  
© The Author(s) 2023

## Abstract

Fatigue-loaded welded constructions are mainly designed according to the experimental results of low-strength steels, although great knowledge about the properties of modern high-strength steels is available. Due to the increasing notch sensitivity with increasing yield strength, the applicable load amplitudes are mostly independent of the steel grade. This paper presents various options for exploiting the potential of high-strength steels subjected to cyclic loads. Therefore, different post-weld treatments are investigated. The calculated fatigue strength is thereby based on IIW guidelines. The results indicate a high potential for an increase in fatigue strength up to a calculated FAT class with a variable slope of FAT392. This is considerably higher than the currently valid base metal level of FAT160.

**Keywords** fatigue strength · post-weld treatment · clean blasting · residual stresses · high-strength steels · weld seam analysis · Tokyo · 2022 · IIW

## 1 Introduction

High-strength steels have become increasingly important in recent years. Due to their high strength, it is possible to design components that are significantly lighter in static areas and still meet the required safety standards.

For cyclically loaded components, the high yield strengths of such steels can only be used profitably in load cases with very high stress ratios. Current guidelines for cyclically loaded components refer to values determined with low-strength steels such as S235 or S355 [1–3]. Therefore, the design of structures is usually limited to a FAT value of 160 MPa. Welded joints are sorted according to the type of joint and stress type, but always far below a FAT160. Since the notch sensitivity in high-strength steels increases with increasing yield strength, the applicable load amplitudes are almost independent of the steel grade if the common welding techniques are kept and no additional treatments

of the finished welds are applied. Critical notches often occur during particular fabrication steps, such as welding. GMAW (gas metal arc welding) is a widely applied process in the industrial environment due to its high deposition rate. However, the resulting weld geometry is unsuitable for components subjected to fatigue loading. Less efficient welding processes, such as TIG welding, have a significantly better weld geometry but much lower deposition rates, which often makes economical use impossible.

The most common way to increase fatigue strength is to apply post-weld treatment methods like remelting the weld toes (TIG-dressing) or mechanical surface treatments like grinding, hammer peening, shot peening, or clean blasting. Various studies have shown that the use of such procedures offers a high potential for improved fatigue strength [4–8].

In this paper, the fatigue strength of the high-strength steels CPW800 and S960QL are investigated based on the improvement of the weld toe geometry and the near-surface material properties by clean blast as a finishing process.

---

Recommended for publication by Commission XIII - Fatigue of Welded Components and Structures.

---

✉ Tom Werner  
to.werner@tu-braunschweig.de

<sup>1</sup> Institute of Joining and Welding, TU Braunschweig, Langer Kamp 8, 38106 Braunschweig, Germany

**Table 1** Mechanical properties of the test materials

Steel	Ultimate tensile strength $R_m$ [MPa]	Yield strength $R_e$ [MPa]	Elongation at break $A$ [%]
S960QL	1052	1010	9.5
CPW800	797	692	16

## 2 Experimental procedure

### 2.1 Materials and welding procedures

The warm-rolled, complex-phase steel CPW800 is used for safety-stressed components in automobile body components. As the CPW800 is utilized predominantly in thin sheet applications, the investigations are carried out on 3.8-mm-thick plates. The high-strength steel S960QL is mainly used for statically loaded components like crane constructions. Here, greater sheet thicknesses are usual. Therefore, the investigations are conducted on 8 mm thickness.

The mechanical properties of both steels are determined by means of tensile tests according to DIN 50,125 [9]. The tests are carried out on at least 3 tensile specimens for each steel. The determining test results are listed in Table 1.

### 2.2 Specimens

The fatigue strength for the CPW800 was investigated at overlap joints, a joint type commonly used in the automotive industry. Therefore, both ends are welded as a full joint. Butt-welded joints are frequently used in crane constructions, which is why these are examined for the S960QL. To keep deviations in the seam geometry as low as possible, all joints were automatically GMA-welded using a welding robot. The size of the welded plates was  $300 \times 500 \text{ mm}^2$ .

Some of the GMA-welded specimens were post-weld treated by re-melting the crack-sensitive weld toes by TIG dressing without filler material (see Table 2). Afterward, the specimens for the fatigue tests were cut out to the dimensions given in Fig. 1 using waterjet cutting.

To remove the roughness caused by water jetting, the sides were grinded. Edges are rounded and provided with compressive residual stresses by polishing.

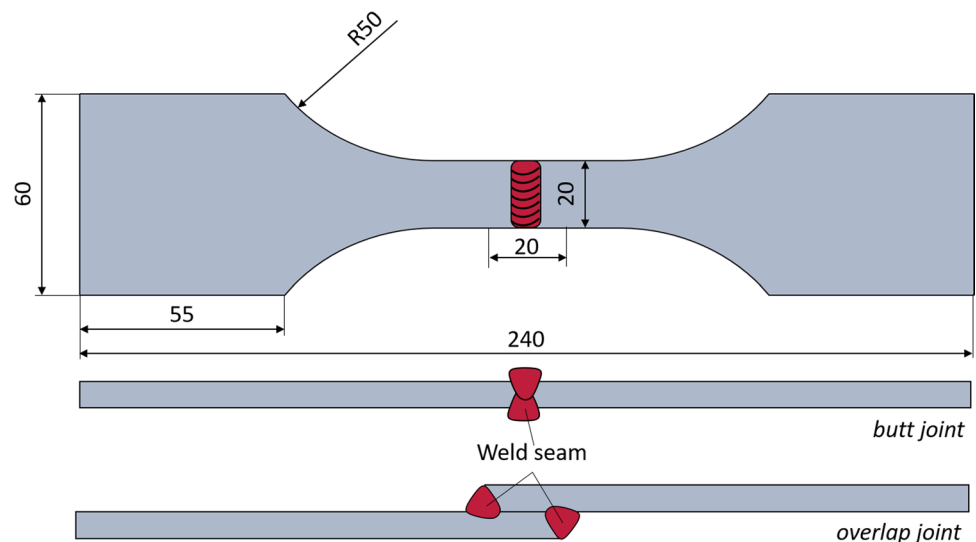
### 2.3 Characterization of the weld seam profile

The weld geometry was determined utilizing laser triangulation. At least three tracks were measured for each weld specimen. The measurement was made from the base material over the weld seam. Recorded values are saved as a point cloud, where  $y$ -coordinates represent the height differences and  $x$ -coordinates the travel distance of the laser. The seam geometry, such as the weld toe angle and the notch radius, are calculated from the determined data of the point clouds. The notch radius was calculated using 3 points, and the seam flank angle using the slope as described at the overlap joint in Fig. 2.

### 2.4 Clean blasting

The post-weld treatment clean blasting was carried out at the S960QL as GMA welded DV-but welds (Fig. 1). The steel shots “S110” (steel shots with a diameter of 0.3–0.6 mm and graphite coated) were used for the cleaning, which was applied at 2 bar. Furthermore, a small area of 2 cm around the seam transition was post-weld treated by clean blasting (Fig. 3).

An active application took place primarily on the upper and lower side of the specimen. Sides were treated secondarily by

**Fig. 1** Specimen geometry

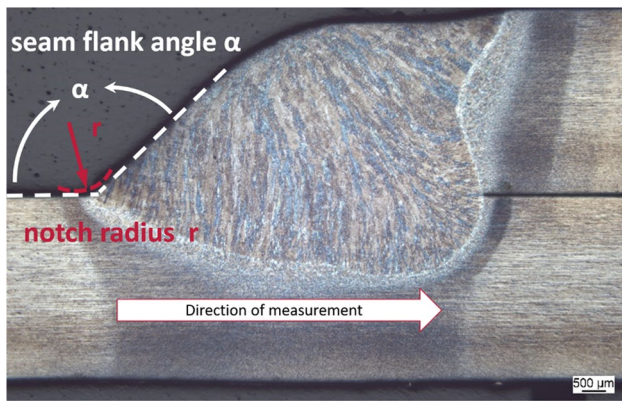


Fig. 2 Definition of the weld geometry (seam flank angel and notch radius)

rebouncing steel shoots. To avoid uneven material behavior, the peening was applied in a continuous movement.

### 2.5 Residual stress determination

The surface residual stresses were determined by X-ray diffraction (XRD) on both sides at the lap joints along a line transverse to the weld (see Fig. 2). The {211} interference lines of the ferrite/martensite were measured for this purpose by means of CrK<sub>α</sub> radiation at 11 incidence angles Ψ. The collimator diameter was 2 mm, and the measurement point spacing was 1 mm. The residual stresses were calculated from the measured interference lines by means of the sin<sup>2</sup> method using the X-ray elastic constant 1/2s<sub>2</sub> = 6.08 · 10<sup>-6</sup> mm<sup>2</sup>/N.

### 2.6 Fatigue tests

The fatigue tests were performed under bending stress using an electromechanical flat-bending torsion machine. The test frequency was uniformly at 25 Hz. Load levels and the evaluation are carried out by using the bead string method according to DIN50100 [3]. To achieve a uniform comparison, the fatigue strength of the nominal stress range (Δσ) was determined at the bending points of the high cycle fatigue line to the endurance limit line for a survival probability P<sub>S</sub> of 97.5% (P<sub>97.5</sub>). A stress ratio of R = 0.1 was used for all the test series. For the evaluation of the tests,

Fig. 3 Clean blasted S960QL specimen

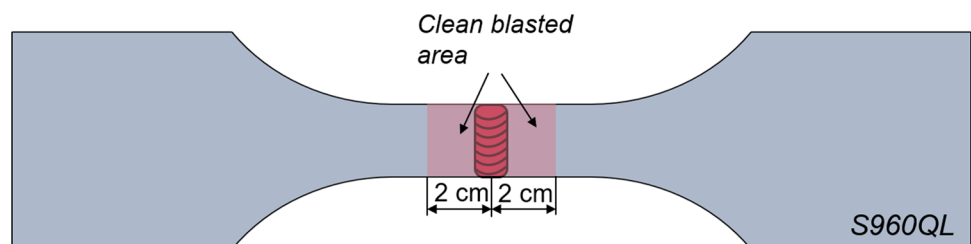


Table 2 Experimental overview of the tested specimens

Steel	GMA welded	GMAW with TIG dressing	GMAW and blast cleaned
S960QL	10	–	13
CPW800	12	15	–

a variable slope *k* is calculated according to Eq. 1. As a measure of the dispersion margin *T<sub>S</sub>* is used. This indicates the confidence range between P<sub>S</sub> = 10% and P<sub>S</sub> = 90% [10].

Calculation of the variable slope:

$$k = \frac{y_2 - y_1}{x_2 - x_1} \tag{1}$$

Dispersion margin:

$$T_s = 1 : ( N_{10\%} / N_{90\%} ) \tag{2}$$

FAT values are calculated based on the determined fatigue strengths at 2 · 10<sup>6</sup> cycles. In this case, a mean stress correction is made according to IIW, and thus the experimental fatigue strength is converted to a stress ratio of R = 0.5. For small specimens, where the residual stresses in the load direction of stress are assumed less than 20% of the yield strength, Eq. 3 is applied according to IIW guidelines [1].

Calculation of the mean stress dependency:

$$f(R) = -0.4 * R + 1.2 \tag{3}$$

Both plates of steel were investigated in the as-welded condition and after a post-weld treatment. The CPW800 steel was additionally TIG-dressed, and the S960QL steel was clean-blasted. Table 2 provides an overview of the test series, including the number of tested samples per test series.

## 3 Results

### 3.1 Weld seam profile analysis

Mean values are formed of the determined weld toe angles and notch radii in order to compare the seam geometries.

**Table 3** Results of the mean seam flank angles and notch radii with standard deviation

Steel	Welding condition	Seam flank angle/sd [°]	Notch radius/sd [mm]
S960QL	TIG dressed	–	–
	As welded	136.2/10.3	1.1/0.4
CPW800	TIG dressed	169.8/4.7	2.5/1.2
	As welded	133.5/20.7	1.3/0.4

The results, including the standard deviations (sd), are shown in Table 3.

The standard deviations in the notch radius of the GMA-welded S960QL specimens are 0.4 mm, and those of the flank angles 10.3°. The standard deviation for the GMA-welded CPW800 is the same.

TIG welding significantly improves the notch geometry. The notch radius increases from 1.3 to 2.5 mm, and the flank angle from 133.5 to 169.8°. Therefore, a great magnitude of both seam geometry parameters (notch radius and seam flank angle) is achieved by TIG dressing.

### 3.2 Residual stress measurements

Since the explicitly performed residual stress measurements at the S960QL are able to verify negligible transverse residual stresses at the weld transition in the as-welded condition, the calculation according to Eq. 3 can be applied (Fig. 4). This approach is also used for the clean-blasted test series containing initial compressive residual stresses since the consideration of residual stresses in the evaluation of the mean stress effect in the IIW concept generally provides only for tensile residual stresses.

As Fig. 5 reveals, the welds contain low compressive residual stresses at the weld toes in the as-welded condition, which is typical for the S960QL steel for the used welding conditions considering the limited size of the used samples. Clean blasting generates an overall higher level of

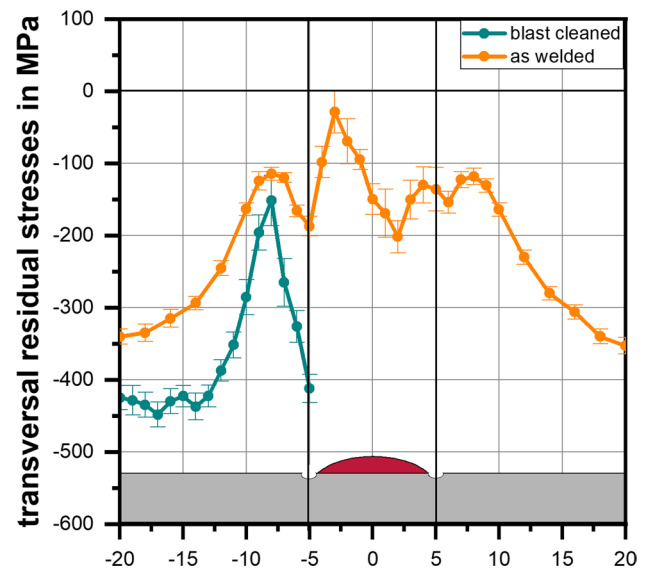


**Fig. 5** Residual stresses in the as-welded condition and after combined post-weld treatment (S960QL)

near-surface compressive residual stresses, with an amount of over  $-400$  MPa at the weld toe (see Fig. 5).

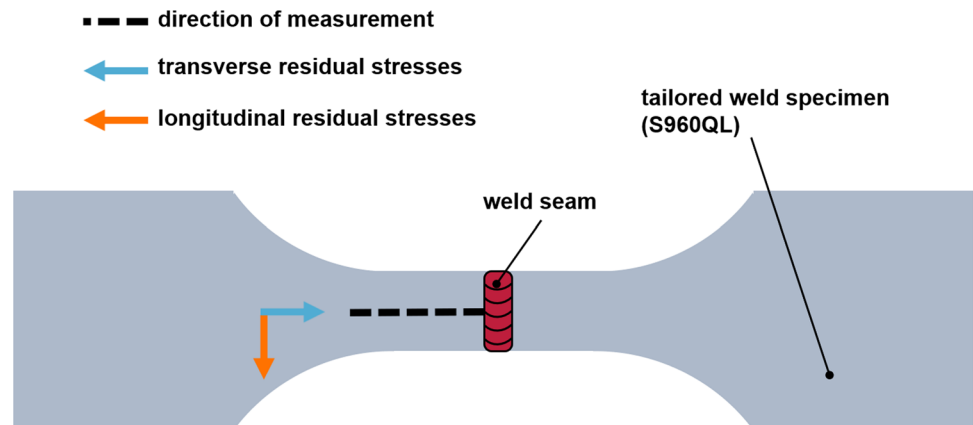
### 3.3 Results of the fatigue tests

The test data are presented in Wöhler diagrams. Full-marked data points present fractured specimens, and not-filled data points present runouts ( $N = 5 * 10^6$ ). Fatigue strength was determined at  $2 * 10^6$  cycles of the  $P_{97.5}$  line. This point is chosen to compare the determined fatigue strength with the current FAT classes.

### 3.4 Initial fatigue strength

Figure 6 illustrates the fatigue test results based on the investigated GMA welded steels, S960QL and CPW800. The weld geometry at the weld seam transition is comparably

**Fig. 4** Measurement sequence for residual stress measurements



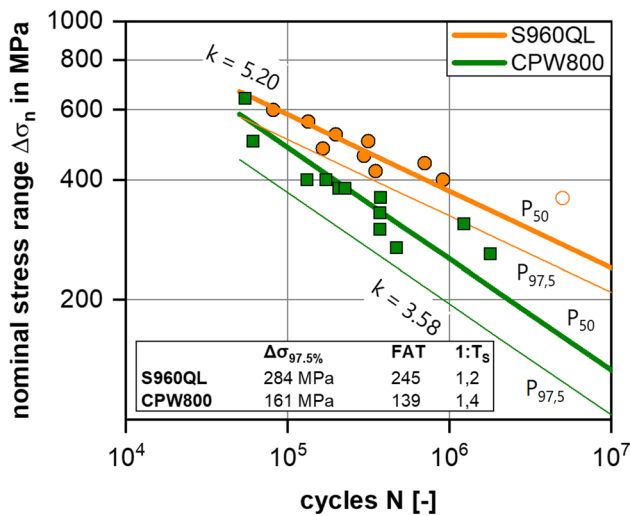


Fig. 6 Initial fatigue strength of high-strength steels

similar for both specimens. All failures were initiated at the weld toe, and no root failures were detected in both test series. The CPW800 specimens already exhibit a fatigue strength of FAT139 and a slope of  $k=3.58$ . An increase is apparent in the higher-strength steel S960QL, where a FAT245 could be determined. Also, the variable slope is increased to a  $k=5.20$  at the S960QL.

### 3.5 Influence of the post-weld treatments

Figure 7 illustrates the effect of weld toe improvement by TIG-dressing of the CPW800 GMA-welds. A noticeable increase in fatigue strength, with a resulting fatigue strength of  $P_{97.5}=407$  MPa to the GMA-welded specimens, is achieved due to the lowered notch sharpness. The mean stress correction

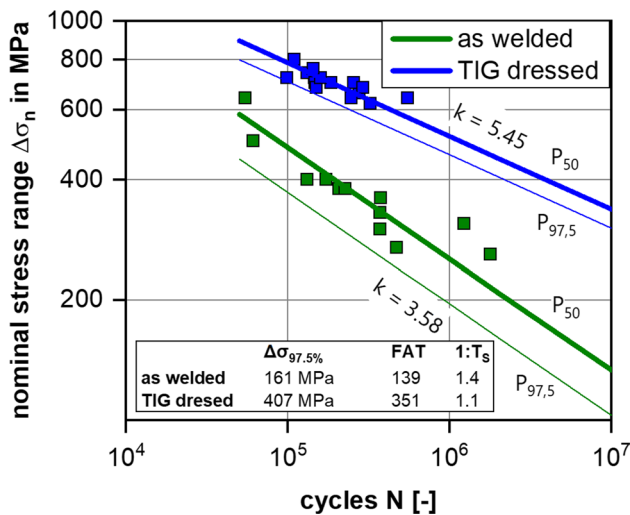


Fig. 7 Influence of TIG dressing on fatigue strength

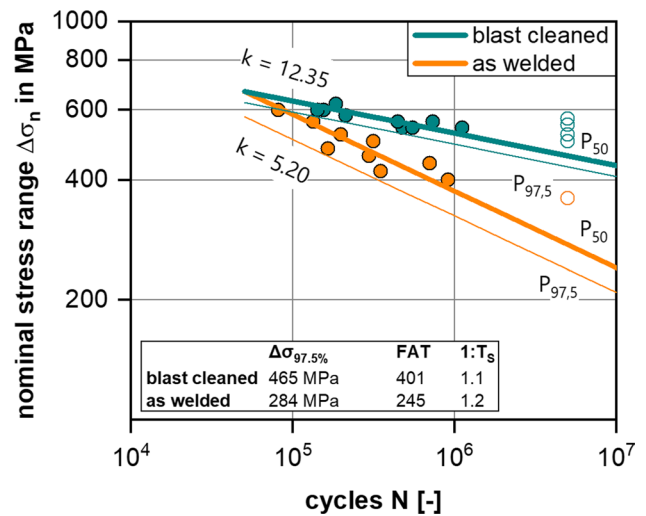


Fig. 8 Influence of blast cleaning on the fatigue strength

results in a related FAT value of 351. The fatigue strength is lower than that of the TIG-welded specimens.

Figure 8 demonstrates the effectiveness of an additional blast cleaning treatment on the example of the GMA-welded S960QL. The resulting FAT value achieved an increase of the fatigue strength by 60% to a calculated FAT401. Furthermore, a great increase in the slope to  $k=12.35$  can be observed. Applied fatigue strength improvement is much more effective with lower stresses than with high stresses, as high stresses overcome the applied compressive residual stresses of the clean blasting. The dispersion of the cycles at a comparable load level can be explained by the strongly flattened slope. It is obvious that the  $S-N$  curve cannot be described perfectly in the range of high cycle fatigue and that the influence of the smallest defects in the specimen or the weld has a great influence on the fatigue strength.

## 4 Conclusions

The results of this investigation demonstrate the great potential of high-strength steel. The fatigue strength of the S960QL with a calculated FAT value of FAT245 is significantly higher than the current standard of FAT90 under axial load. Also, the CPW800 is with FAT139 remarkably above the current limit for an overlap joint (FAT63). Due to the determined notch stress situation, the higher yield strength influences obviously the resulting fatigue strength. Both presented results of the indicated  $S-N$  curves a more sophisticated evaluation of the fatigue behavior should be given to high-strength steels in current standards. The post-weld treatments of the investigated joints also demonstrate a currently too-low considered improvement of the fatigue strength.

A correlation between weld geometry and fatigue strength indicates the examined test series of TIG-dressed specimens, as illustrated in Fig. 8. In addition to the increased fatigue strength, a flattening of the Wöhler curve in the high cycle strength range can also be observed. Due to the improvement of the weld seam geometry, the fatigue strength of the CPW800 welds could be increased by 140% to a FAT351. Great industrial potential for this post-treatment method is especially in thick plates. Thus, the high efficiency of the GMA welding can be utilized in multilayer welds with an improved fatigue strength of the TIG dressing. This post-weld treatment combines a considerable increase in fatigue strength with the efficiency of the GMA welding.

Another approach to increase the fatigue strength of high-strength steels is clean blasting with sufficient intensity. With this post-weld treatment method, the weld toe geometry is not influenced, but the effects of hardening and the generation of compressive residual stresses are exploited. Accompanying cold hardening processes were not explicitly examined in these experiments but can be assumed on the basis of existing experiments [11, 12]. The results show an increase in the fatigue strength for the GMA-welded and clean-blasted samples of the steel S960QL up to a FAT401. Probably still higher fatigue strength may be expected with an additionally improved weld seam geometry. However, it is apparent that the clean blasting treatment and the associated boundary layer changes, in particular the generation of compressive residual stresses close to the surface, can largely compensate for the remaining notch effect of the already optimized seam transitions. The increase primarily takes effect in the high cycle range. These differences decrease in the low cycle range, which may be due to a partial relaxation of the compressive residual stresses, as commonly expected when the upper stresses become almost as high as the yield strength.

In order to obtain the full potential of the clean blasting treatment, the samples must be checked thoroughly for defects. However, a clear increase in fatigue strength can be identified in all cases.

The small number of test samples must be considered in the results obtained. With a larger scope of experiments, the fatigue strengths of the steels could change. A statistical validation can therefore not perfectly be given. Furthermore, the load type must be considered well. All the tests have been performed under a bending load. A lower fatigue strength under an axial load of the same samples is assumed.

**Acknowledgements** The presented research is being founded by two AiF projects: “Nutzung von Potentialen höherfester Stähle durch Schweißprozessoptimierung und Entwicklung neuer lokaler Bemessungskonzepte (IGF-Nr. 20.366 BG/2)” and “Optimierungsstrategien

für die Maximierung der Schwingfestigkeit schwingbeanspruchter Schweißkonstruktionen aus höchstfesten Stählen und deren Berücksichtigung in den Bemessungsrichtlinien (IGF-Nr. 21720 N).” We also want to thank the DVS who supported this trip within the “Young Professional” program.

**Funding** Open Access funding enabled and organized by Projekt DEAL.

## Declarations

**Conflict of interest** The authors declare no competing interests.

**Open Access** This article is licensed under a Creative Commons Attribution 4.0 International License, which permits use, sharing, adaptation, distribution and reproduction in any medium or format, as long as you give appropriate credit to the original author(s) and the source, provide a link to the Creative Commons licence, and indicate if changes were made. The images or other third party material in this article are included in the article's Creative Commons licence, unless indicated otherwise in a credit line to the material. If material is not included in the article's Creative Commons licence and your intended use is not permitted by statutory regulation or exceeds the permitted use, you will need to obtain permission directly from the copyright holder. To view a copy of this licence, visit <http://creativecommons.org/licenses/by/4.0/>.

## References

- Hobbacher A (1996) Fatigue design of welded joints and components: recommendations of IIW Joint Working Group XIII - XV. Woodhead Publishing
- Kuhlmann U, Feldmann M, Lindner J, Müller C, Stroetmann R, eds. (2014) ‘Eurocode 3 Bemessung und Konstruktion von Stahlbauten’ 1st edn. Beuth; Ernst, Berlin, Wien, Zürich, Berlin
- ‘DIN 50100:2016–12, Schwingfestigkeitsversuch\_ - Durchführung und Auswertung von zyklischen Versuchen mit konstanter Lastamplitude für metallische Werkstoffproben und Bauteile’
- Marquis GB, Mikkola E, Yildirim HC, Barsoum Z (2013) Fatigue strength improvement of steel structures by high-frequency mechanical impact: proposed fatigue assessment guidelines. *Weld World* 57(6):803–822
- Duchet M, Haouas J, Gibeau E et al (2019) Improvement of the fatigue strength of welds for lightweight chassis application made of advanced high strength steels. *Procedia Struct Integr* 19:585–594
- Pedersen MM, Mouritsen OØ, Hansen MR, Andersen JG, Wenderby J (2010) Comparison of post-weld treatment of high-strength steel welded joints in medium cycle fatigue. *Weld World* 54(7–8):R208–R217
- Lieurade HP, Huther I, Lefebvre F (2008) Effect of weld quality and postweld improvement techniques on the fatigue resistance of extra high strength steels. *Weld World* 52(7–8):106–115
- Wohlfahrt H, Krull P. (2000) ‘Mechanische Oberflächenbehandlungen: Grundlage-Bauteileigenschaften-Anwendungen’ Weinheim, Germany
- ‘DIN 50125:2016–12, Prüfung metallischer Werkstoffe\_ - Zugproben’
- Haibach E (1992) Betriebsfeste Bauteile: Ermittlung und Nachweis der Betriebsfestigkeit, konstruktive und unternehmerische Gesichtspunkte. Springer-Verlag, Berlin, New York
- Efremov D, Gerasimova A (2021) Shotblasting process for surface hardening. *Mat Today: Proc* 38:1685–1688
- Mechanische Oberflächenbehandlungen: (2000) Grundlage-Bauteileigenschaften-Anwendungen’

**Publisher's note** Springer Nature remains neutral with regard to jurisdictional claims in published maps and institutional affiliations.